Available online at www.sciencedirect.com
SCIENCE DIRECT®
Journal of the European Ceramic Society 25 (2005) 3173–3179
www.elsevier.com/locate/jeurceramsoc

Fabrication of low thermal expansion porous body of cubic cesium-deficient type pollucite

Ikuo Yanase*, Sachiko Tamai, Shuzo Matsuura, Hidehiko Kobayashi

Department of Applied Chemistry, Faculty of Engineering, Saitama University, 255 Shimo-ohkubo, Sakura-ku, Saitama 338-8570, Japan

Received 5 April 2004; received in revised form 14 June 2004; accepted 26 June 2004
Available online 12 September 2004

Abstract

Porous bodies of cubic Cs-deficient pollucite, $Cs_{0.9}Al_{0.9}Si_{2.1}O_6$, were fabricated by using pollucite-calcined powder and polymethyl methacrylate (PMMA), as a pore-forming agent. Porous structure with 0.37 μm in pore-size and 48.4% in porosity was obtained by heating the green compact of the 1073 K-calcined powder including 35 mass% PMMA at 873 K in air for 20 h to decompose PMMA, following at 1673 K in air for 20 h. The porous structure was formed via the process that small pores resulted from the PMMA decomposition, enlarged and grain growth occurred together with the neck formation with increasing the heating temperature. The fabricated $Cs_{0.9}Al_{0.9}Si_{2.1}O_6$ porous body had the low thermal expansion property of which the linear thermal expansion coefficient was ca. $1.0 \times 10^{-6}\,K^{-1}$ in the temperature range of 298–1273 K.

Keywords: Porous structure; Pollucite; PMMA; Thermal expansion; $CsAlSi_2O_6$

1. Introduction

In recent years, ceramic filters have been developing for removal of small particles in polluted air originating mainly from vehicular traffic and energy production under higher temperatures, and many studies on porous materials for filtering hot gas have been reported.[1–6] However, porous materials used and studied, have a serious problem that microcracks arise from thermal stress due to anisotoropic thermal expansion in case of using the materials in high-temperature environments.[7] For instance, the cordierite ceramic honeycombs have an issue that microcracks occur during regeneration.[8] As one of solution methods for such the problems, it is thought that application of substances with cubic symmetry and low thermal expansion properties for hot gas-filter materials.

Pollucite, $CsAlSi_2O_6$, cubic with space group of *Ia*-3*d*, has a three-dimensional aluminosilicate framework structure of 48 $(Si,Al)O_4$ tetrahedra and 16 Cs^+ ions in 12-coordinated sites surrounded by the framework.[9] Lattice parameter of pollucite is around 1.3678 nm[10–12] and melting point >1900 K.[13] There are many reports[9–12,14] on thermal expansion properties for pollucites. Thermal expansion coefficient (TEC) above 473 K of pollucite is very low; TEC values were in range of 0 to $2 \times 10^{-6}\,K^{-1}$. However, the TEC in temperature range of RT to 473 K is very high; TEC values 10 to 20 $\times 10^{-6}\,K^{-1}$. In our previous study,[10,14] cubic Cs-deficient type pollucite powder, $Cs_{0.9}Al_{0.9}Si_{2.1}O_6$, was synthesized by the multi-step heat treatment. TEC values for the synthesized $Cs_{0.9}Al_{0.9}Si_{2.1}O_6$ were around $2.0 \times 10^{-6}\,K^{-1}$ in temperature range of 298–1273 K.[10,14] And further we succeeded to fabricate the dense sintered body of $Cs_{0.9}Al_{0.9}Si_{2.1}O_6$ showing low thermal expansion by using amorphous pollucite-calcined powders with size <100 nm in particle diameter.[15]

From the described above, it is thought that application of cubic Cs-deficient type pollucite to a novel low-thermal expansion porous material. Considering the pollucite-sintered bodies have been fabricated by using the amorphous powders with small particles <100 nm,[15] it would be expected

* Corresponding author. Tel.: +81 48 858 3720; fax: +81 48 858 3720.
E-mail address: yanase@apc.saitama-u.ac.jp (I. Yanase).

0955-2219/$ – see front matter © 2004 Elsevier Ltd. All rights reserved.
doi:10.1016/j.jeurceramsoc.2004.06.020

that submicron-porous materials could be fabricated by utilizing the fine powders and pore-forming agents, and further, it could be candidates for filtering fine particles with a diameter <1 μm arising from the secondary combustion products from vehicular traffic and energy production.[16–18]

In this work, cubic $Cs_{0.9}Al_{0.9}Si_{2.1}O_6$ porous bodies with submicron-pores have been fabricated using $Cs_{0.9}Al_{0.9}Si_{2.1}O_6$ calcined powders and PMMA as a pore-forming agent. And then, the porous specimens have been investigated by a scanning electron microscopy, an Hg-intrusion method, and a thermal mechanical analysis.

2. Experimental

2.1. Synthesis of $Cs_{0.9}Al_{0.9}Si_{2.1}O_6$ powder

$CsNO_3$ powder (99% up; Koujyundo Kagaku Co., Ltd., Japan), Al_2O_3 sol (Alumina sol 200; Nissan Kagaku Co., Ltd., Japan) and SiO_2 sol (Snotex O; Nissan Kagaku Co., Ltd., Japan) were used as starting raw materials. Firstly, Al_2O_3 and SiO_2 sols were mixed at pH 5.4, dried, and heated at 873 K in air for 20 h to obtain mixed fine powders of γ-Al_2O_3 and amorphous SiO_2 (molar ratio of Al/Si = 0.9/2.1).[19] Secondary, $CsNO_3$ powders were added to the fine powder mixtures of γ-Al_2O_3 and amorphous SiO_2 to give the molar ratio of 0.9/2.1 for Cs/Si. The mixed powders were heated at 873 K in air for 20 h to decompose $CsNO_3$. Then, the powders were calcined at each temperature of 923 to 1273 K in air for 20 h, in order to synthesize calcined powders with chemical composition of $Cs_{0.9}Al_{0.9}Si_{2.1}O_6$.

2.2. Fabrication of $Cs_{0.9}Al_{0.9}Si_{2.1}O_6$ porous body

Firstly, polymethyl methacrylate (PMMA; $(C_5H_8O_2)_n$, ca. 2–3 mm particles, Wako Co., Ltd., Japan), was dissolved in acetone by ultrasonic treatment to prepare PMMA solution, and then the calcined powders of $Cs_{0.9}Al_{0.9}Si_{2.1}O_6$, previously dispersed in acetone for 10 min by ultrasonic treatment, were mixed with PMMA in the solution for 20 h by ball milling. Mixing ratio of PMMA to the calcined powders was in range of 0–50 mass%. Then the acetone was removed from the slurry with an evaporator, and the dried mixtures consist of the calcined powders and PMMA, were used for green compacts.

Green compacts composed of the calcined powders and PMMA were prepared by anisotropic pressing at 49 MPa for 1 min, followed by cold isostatic pressing (CIP) at 196 MPa for 1 min. The specimen size was approximately 5 mm × 5 mm × 10 mm. The prepared compact was heated at 873 K in air for 20 h to remove PMMA, with heating rate of 2 K/min. Here the temperature for deleting PMMA was determined from the result that PMMA was decomposed in temperature range of 573–773 K, investigated by TG-DTA. Then the preheated specimens were sintered at 1673 K in air for 20 h to fabricate porous bodies of $Cs_{0.9}Al_{0.9}Si_{2.1}O_6$.

2.3. Evaluations

Specific surface areas of the calcined powders were investigated using nitrogen adsorption apparatus (Sorptmatic 1990; CE Instruments Corp.). Crystalline phases in the calcined powders and the $Cs_{0.9}Al_{0.9}Si_{2.1}O_6$ porous bodies were examined by X-ray diffraction apparatus (XRD; Rad-B, Rigaku Co., Ltd., Japan, Cu Kα, 40 kV, 30 mA). Morphologies and particle distribution for the calcined powders and fractured surfaces of the porous bodies were observed using a scanning electron microscope (SEM; S-4100, Hitachi Co., Ltd., Japan).

Relative densities of the fabricated $Cs_{0.9}Al_{0.9}Si_{2.1}O_6$ porous bodies were calculated from bulk densities measured by the Archimedes' method using water. Here, theoretical density of $Cs_{0.9}Al_{0.9}Si_{2.1}O_6$ was 3.10 g/cm^3, which were calculated from lattice volume for the synthesized $Cs_{0.9}Al_{0.9}Si_{2.1}O_6$ powder by a least squared method.[10] Porosity and pore-size distribution for the $Cs_{0.9}Al_{0.9}Si_{2.1}O_6$ porous bodies were investigated using an Hg-intrusion porosimetry (Autopore 9520, Shimadzu Co., Ltd., Japan). Thermal behaviours for the green compact of $Cs_{0.9}Al_{0.9}Si_{2.1}O_6$ and thermal expansion properties for the porous bodies of $Cs_{0.9}Al_{0.9}Si_{2.1}O_6$ in temperature range of 298–1273 K were investigated using a thermal mechanical analyzer (TMA; Thermoflex, Rigaku Co., Ltd., Japan).

3. Results and discussion

3.1. Characterization of $Cs_{0.9}Al_{0.9}Si_{2.1}O_6$ calcined powders and green compacts

XRD patterns for the powders obtained by heating the mixed raw materials at 923, 1073 and 1273 K in air for 20 h, are shown in Fig. 1a–c, respectively. An amorphous phase was recognized in the powder calcined at 923 K (923 K-calcined powder), and crystalline pollucite and slight amorphous phases were recognized in the powder calcined at 1073 K (1073 K-calcined powder). Single phase of pollucite with a well-crystallized phase was recognized in the powder calcined at 1273 K (1273 K-calcined powder). SEM photographs for the 923, 1073, and 1273 K-calcined powder in air for 20 h are shown in Fig. 1A–C, respectively. From the SEM photographs, it was observed that particle growth and aggregation progressed with increasing the calcination temperature. And also specific surface areas for these calcined powders decreased with increasing the temperature.

Thermal behaviours of the green compacts without PMMA, fabricated using the 923, 1073, and 1273 K-calcined powder, were investigated by the TMA. The results are shown in Fig. 2. And SEM images of the fractured surfaces of the specimens fabricated by heating the compact of the 923, 1073, and 1273 K-calcined powder at 1673 K in air for 5 h, are shown in Fig. 2b–d, respectively.

In case of the 1273 K-calcined powders, the compact expanded in the temperature range of RT to 1273 K. The

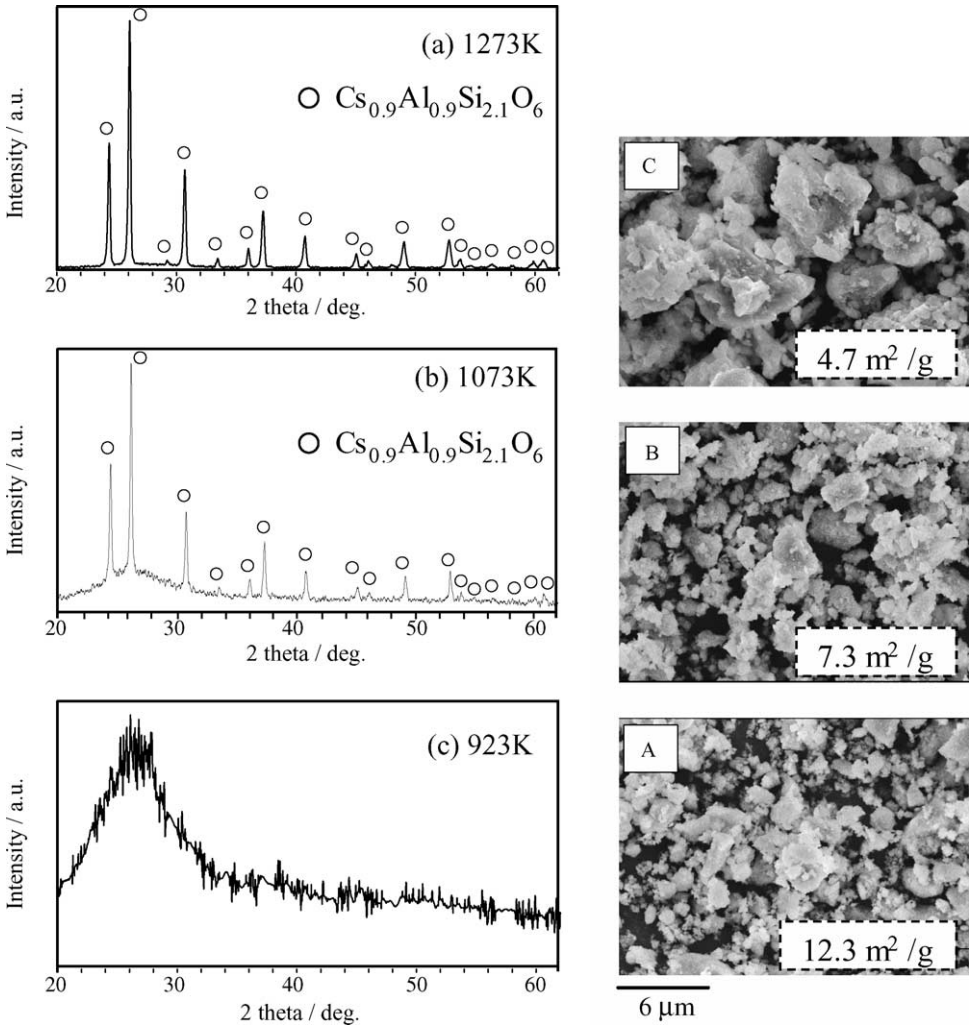

Fig. 1. XRD patterns and SEM photographs for the powders calcined at 923 K (a), 1073 K (b) and 1273 K (c) in air for 20 h.

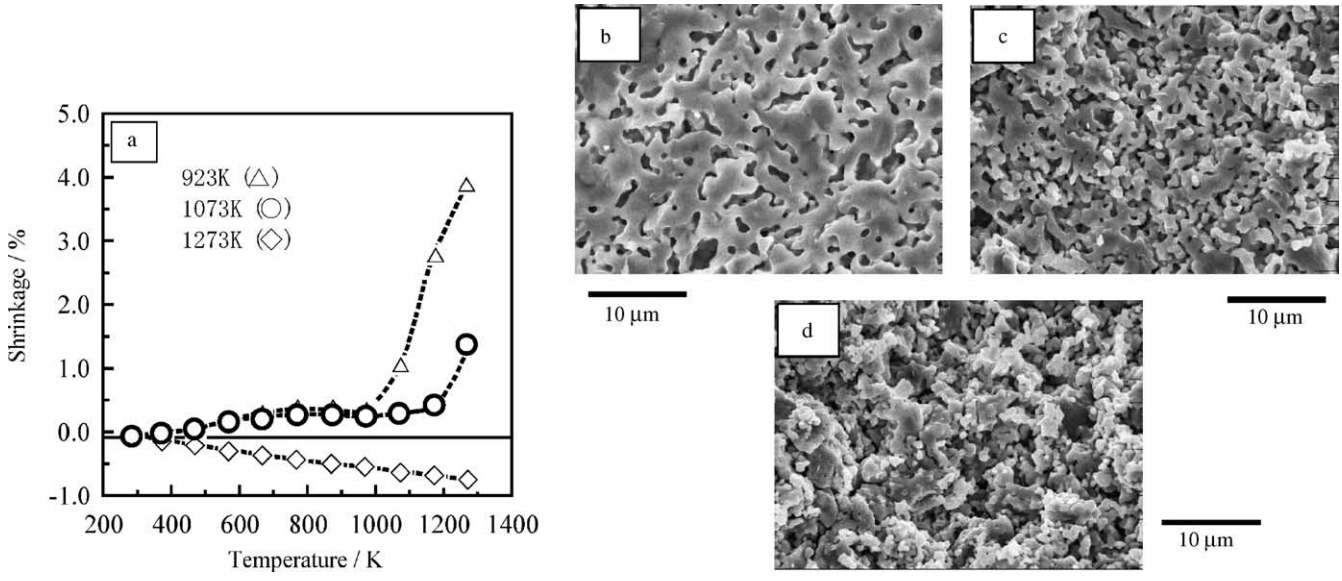

Fig. 2. Thermal behaviours (a) of the compacts fabricated using the powders calcined at 923, 1073, and 1273 K in air for 20 h. And SEM images for the fractured surfaces for the specimens using the (b) 923 K-calcined, (c) 1073 K-calcined, and (d) 1273 K-calcined powders.

expansion seemed to be due to the particle growth and aggregation as shown in Fig. 1c. From the SEM image shown in Fig. 2d, the small particles were clearly observed because the sintering was suppressed. Contrary, the compact for the 923 K-calcined powders showed a slow shrinkage in the temperature range of RT to ca. 923 K and showed a rapid shrinkage above 923 K, corresponding to the calcination temperature 923 K. This result suggests that particles growth in the 923 K-calcined powder rapidly proceeded due to the higher specific surface area. From the SEM image shown in Fig. 2b, it was recognized that the sintering among particles significantly progressed. Similarly, in case of the 1073 K-calcined powders, the compact apparently showed a shrinkage above ca. 1073 K, corresponding to the calcination temperature 1073 K. However, the shrinkage was smaller than the case of the 923 K-calcined powder. As a result, pore formation and particle growth occurred in the fractured surface of the specimen for the 1073 K-calcined powder from the SEM image in Fig. 2c.

Relationship between the calcination temperatures and relative densities for the fabricated $Cs_{0.9}Al_{0.9}Si_{2.1}O_6$ specimens is shown in Fig. 3. The relative densities decreased from 69.4 to 56.0% with increasing calcination temperature from 923 to 1273 K. The specimen for the 1273 K-calcined powder had a lowest relative density because of the aggregation and the particle growth in the powder. The specimen of the 923 K-calcined powder had the highest relative density due to fine particle powders with higher specific surface area. In case of the 1073 K-calcined powder, the specimens had a low relative density compared to the case of the 923 K-calcined powder.

From the results for Figs. 2 and 3, it was found that using 1073 K-calcined powders was appropriate for forming pore structure and increasing the pore volume in the $Cs_{0.9}Al_{0.9}Si_{2.1}O_6$ specimens.

3.2. Fabrication of $Cs_{0.9}Al_{0.9}Si_{2.1}O_6$ porous body

In order to examine the effective adding amount of PMMA for fabrication of porous structure in the $Cs_{0.9}Al_{0.9}Si_{2.1}O_6$ specimens, relationship between the amounts of PMMA addition and the relative densities for the specimens was investigated. Here, all the $Cs_{0.9}Al_{0.9}Si_{2.1}O_6$ specimens were fabricated by heating the green compacts of the 1073 K-calcined powder containing PMMA at 873 K in air for 24 h, followed by sintering at 1673 K in air for 20 h. The 1073 K-calcined powders used for the compacts, were previously dispersed by the ultrasonic treatment. The obtained result is shown in Fig. 4. The relative density decreased from 72.5 to 42.6% with increasing the PMMA amount of 0 to 50 mass% because PMMA volume in the green compacts increased. The result shows that pore volume in the fabricated $Cs_{0.9}Al_{0.9}Si_{2.1}O_6$ specimen increases with increasing the amount of PMMA.

SEM photographs for the fractured surfaces of the $Cs_{0.9}Al_{0.9}Si_{2.1}O_6$ specimens fabricated by heating the compacts containing 35 mass% PMMA at 1373, 1473, 1573 and 1673 K in air for 20 h, are shown in Fig. 5a–d, respectively. From Fig. 5a, it was observed that both sizes of the particles and the pores were below ca. 0.5 μm, and grain growth hardly enhanced at 1373 K. In case of 1473 and 1573 K, the grains and pores in the specimens apparently enlarged with increasing the heating temperature, as shown in Fig. 5b and c. And in case of 1673 K, the porous structure with pores of size around 0.5 μm was formed, together with the grain growth and the neck formation, as shown in Fig. 5d. From these SEM images, it was clarified that the formations of such porous structures were progressed as follows. Firstly, the microstructure in the $Cs_{0.9}Al_{0.9}Si_{2.1}O_6$ specimens was formed at 1373 K, resulting from the PMMA decomposition at 873 K for 20 h. Secondary, the pores enlarged and the grain growth enhanced with increasing the heating temperature. Finally, the $Cs_{0.9}Al_{0.9}Si_{2.1}O_6$ porous body with the porous structure was fabricated at 1673 K.

Particle distribution for the 1073 K-calcined powders dispersed by the ultrasonic treatment is shown in Fig. 6, investigated from SEM image, on right-upper side in the Fig. 6, showing morphology for the 1073 K-calcined powder. The particles were mainly in range of 0.3–0.5 μm in diameter. Effect of the ultrasonic treatment on the parti-

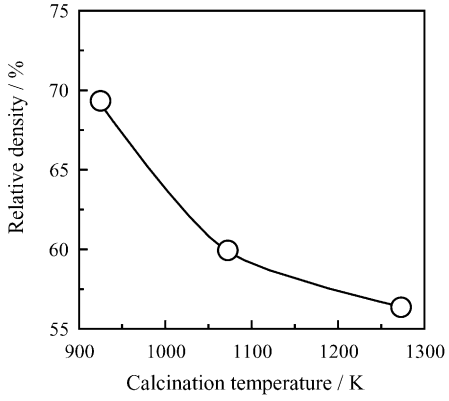

Fig. 3. Effect of calcination temperature on relative density of the $Cs_{0.9}Al_{0.9}Si_{2.1}O_6$ specimens.

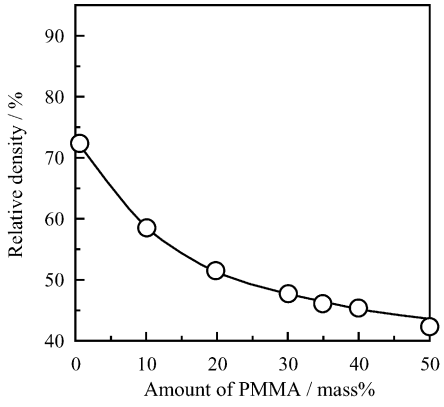

Fig. 4. Relationship between amount of PMMA addition and the relative density of the porous specimens.

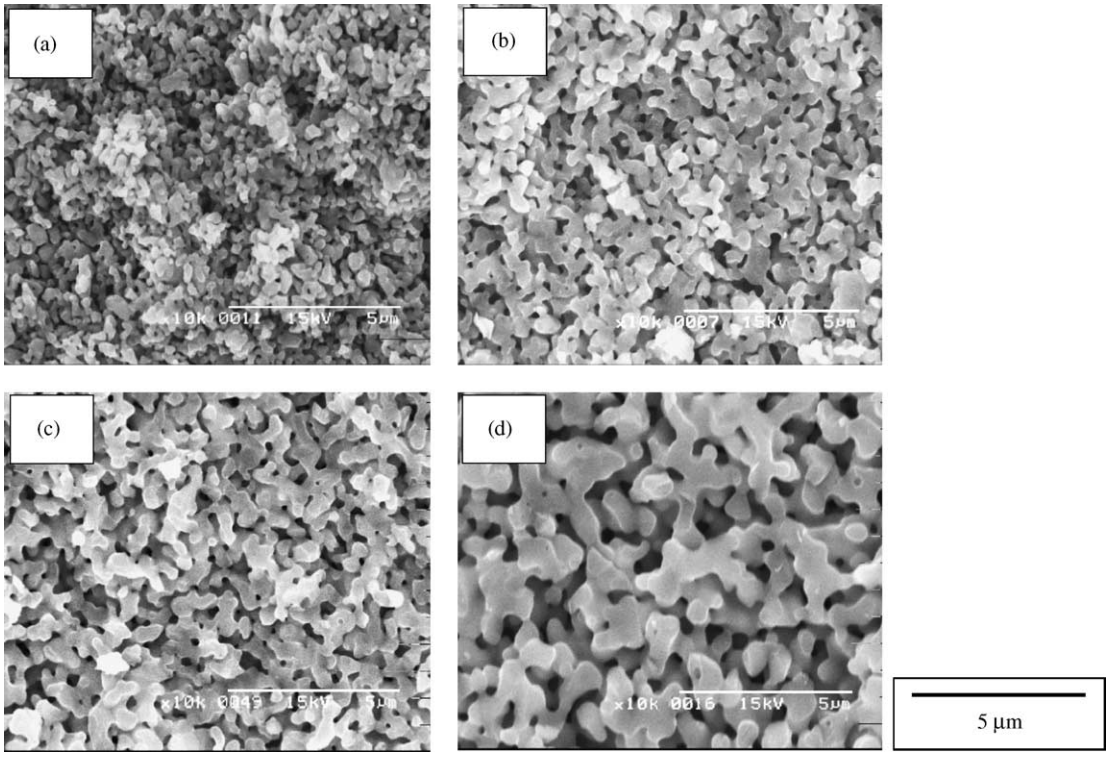

Fig. 5. SEM photographs for the fractured surface of the $Cs_{0.9}Al_{0.9}Si_{2.1}O_6$ porous bodies fabricated by sintering at 1373 K (a), 1473 K (b), 1573 K (c) and 1673 K (d) in air for 20 h.

cle dispersion was clearly recognized in comparison with the 1073 K-calcined powder as prepared without the ultrasonic treatment, shown in Fig. 1b, though aggregation was also observed among the particles in the SEM image of Fig. 6.

Therefore, it was considered that the dispersed particles influenced on formation of the small pores in the specimens at 1373 K, as shown in Fig. 5a. That is, the microstructure with homogeneous small pores would be obtained when the calcined powders could be well dispersed and well mixed with the PMMA solution.

3.3. Pore structure and thermal expansion of $Cs_{0.9}Al_{0.9}Si_{2.1}O_6$ porous body

Pore-size distribution for the $Cs_{0.9}Al_{0.9}Si_{2.1}O_6$ porous body fabricated at 1673 K is shown in Fig. 7. Pores of 0.37 μm in diameter were mainly observed in the porous body, of

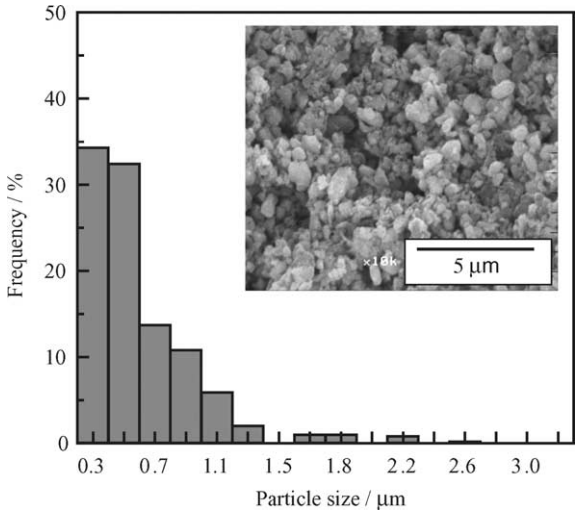

Fig. 6. Particle-size distribution for the 1073 K-calcined powder performed by ultrasonic treatment and SEM image on right-upper side is morphology for the powder.

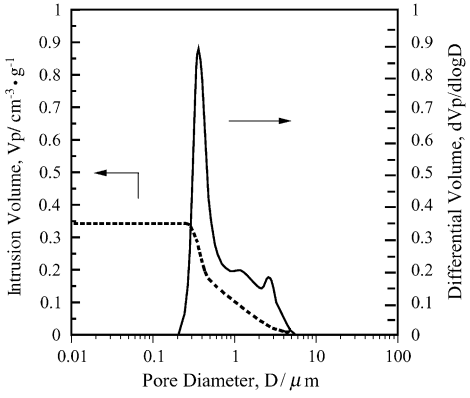

Fig. 7. Pore-size distribution for the $Cs_{0.9}Al_{0.9}Si_{2.1}O_6$ porous bodies fabricated using 1073 K-calcined powder and 35 mass% PMMA.

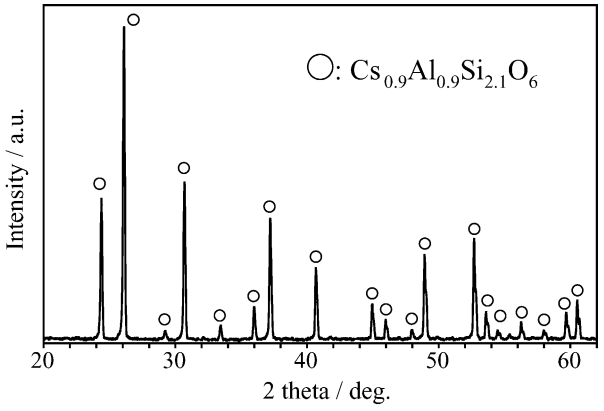

Fig. 8. XRD pattern of the fabricated $Cs_{0.9}Al_{0.9}Si_{2.1}O_6$ porous body.

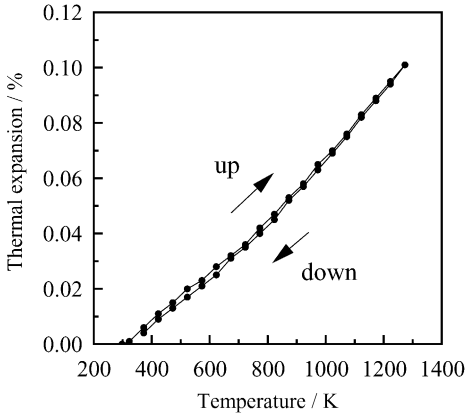

Fig. 9. Thermal expansion behaviour of the fabricated $Cs_{0.9}Al_{0.9}Si_{2.1}O_6$ porous body in the temperature range of 298–1273 K.

which the differential volume was much larger than pores of 2.60 μm slightly observed in the same specimen. Porosity of the specimen was 48.4%. Thus, it was found that the porous structure with almost homogeneous submicron-pores was fabricated by mixing the 1073 K-calcined powders dispersed and the PMMA solution of optimum amount 35 mass%, using the ball milling.

XRD pattern for the fractured surface of the $Cs_{0.9}Al_{0.9}Si_{2.1}O_6$ porous body fabricated by using the 1073 K-calcined powders and 35 mass% PMMA is shown in Fig. 8.

Crystalline phase for the porous body was $Cs_{0.9}Al_{0.9}Si_{2.1}O_6$ single phase without a glassy phase, referring to the JCPDS card (No. 29-0407) for $CsAlSi_2O_6$. And it was found that the $Cs_{0.9}Al_{0.9}Si_{2.1}O_6$ phase was completely crystallized at 1673 K via the formation of the porous structure, considering that the 1073 K-calcined powder included the amorphous phase, used for the green compact.

Thermal expansion behaviour in the temperature range of 298–1273 K for the $Cs_{0.9}Al_{0.9}Si_{2.1}O_6$ porous body

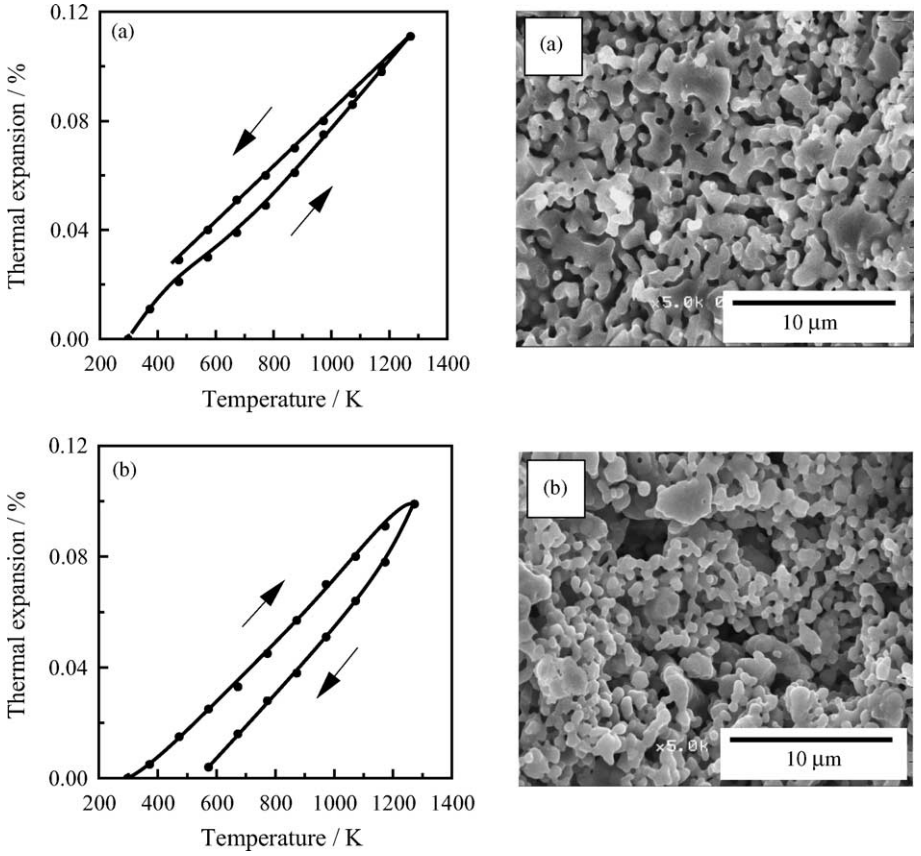

Fig. 10. Thermal expansion behaviours and fractured surfaces of the $Cs_{0.9}Al_{0.9}Si_{2.1}O_6$ porous bodies fabricated using 20 mass% (a) and 50 mass% PMMA (b).

fabricated using the 1073 K-calcined powder and 35 mass% PMMA, was investigated by the TMA referring to the fused silica. The result is shown in Fig. 9. The porous body showed almost linear thermal expansion property of which the thermal expansion rate was 0.101% and the TEC was $1.0 \times 10^{-6}\,K^{-1}$. In addition, a hysteresis was not recognized in the property with increasing and decreasing temperature.

On the other hand, in Fig. 10, thermal expansion behaviours and fractured surfaces for the $Cs_{0.9}Al_{0.9}Si_{2.1}O_6$ porous bodies fabricated using 1073 K-calcined powder and of 20 mass% PMMA and 50 mass% PMMA were shown together. In case of 20 mass% PMMA, pores formation were not enough in the specimens because amount of PMMA was too small, and a hysteresis was recognized in the thermal expansion behaviour. In case of 50 mass% PMMA, it was observed that necks among particles were not formed enough due to much larger amount of PMMA, and that a huge hysteresis in the thermal expansion behaviour. Therefore, it was thought that such hystereses were due to the heterogeneous microstructures in the specimens.

From the results of Figs. 9 and 10, it was found that the thermal expansion behaviours for the $Cs_{0.9}Al_{0.9}Si_{2.1}O_6$ porous bodies were significantly influenced by the added amount of PMMA, and that it was important for homogeneous porous structures to clarify the optimum amount of PMMA.

4. Conclusions

Obtained results in this study on fabrication and thermal expansion properties for Cs-deficient type pollucite porous bodies were described as follows:

(1) $Cs_{0.9}Al_{0.9}Si_{2.1}O_6$ porous bodies were fabricated by heating green compacts of powder mixtures prepared by mixing 1073 K-calcined powders and PMMA dissolved in acetone, at 873 K in air for 20 h and followed by at 1673 K in air for 20 h.
(2) The PMMA was removed from the green compacts by heating at 873 K for 20 h. The porous structures of the $Cs_{0.9}Al_{0.9}Si_{2.1}O_6$ specimens were formed by grain growth and neck formation with increasing the heating temperature to 1673 K.
(3) In case of using the 1073 K-calcined powder and the 35 mass% PMMA, porous structure with 0.37 μm in size and 48.4% in porosity, was obtained in the fabricated $Cs_{0.9}Al_{0.9}Si_{2.1}O_6$ porous body.
(4) The $Cs_{0.9}Al_{0.9}Si_{2.1}O_6$ porous body had the low thermal expansion property of which the linear thermal expansion coefficient was ca. $1.0 \times 10^{-6}\,K^{-1}$ in temperature range of 298–1273 K.

References

1. Fernando, J. A. and Chung, D. D. L., Pore structure and permeability of alumina fiber filter membrane for hot gas filteration. *J. Porous Mater.*, 2002, **9**, 219–222.
2. Alves, H. M., Tari, G., Fonseca, A. T. and Ferreira, J. M. F., Processing of porous cordierite bodies by starch consolidation. *Mater. Res. Bull.*, 1998, **33**, 1439–1448.
3. Park, J. K., Lee, J. S. and Lee, S. I., Preparation of porous cordierite using method and its feasibility as a filter. *J. Porous Mater.*, 2002, **9**, 203–210.
4. Fernando, J. A. and Chung, D. D. L., Improving an alumina fiber filter membrane for hot gas filtration using an acid phosphate binder. *J. Mater. Sci.*, 2001, **36**, 5079–5085.
5. Jo, Y. M., Hutchison, R. B. and Raper, J. A., Characterization of ceramic composite membrane filters for hot gas cleaning. *Powder Tech.*, 1997, **91**, 55–62.
6. Das, N. and Maiti, H. S., Formation of pore structure in tape-cast alumina membranes—effects of binder content and firing temperature. *J. Membr. Sci.*, 1998, **140**, 205–212.
7. Kamiya, H., Sekiya, Y. and Horio, M., Thermal stress fracture of rigid ceramic filter due to char combustion in collected dust layer on filter surface. *Powder Tech.*, 2001, **115**, 139–145.
8. Matsunuma, K., Ihara, T., Ban, S., Nakajima, S. and Okamoto, S., Development of porous metal diesel particulate filter. *JSAE Rev.*, 1999, **16**, 312.
9. Richerson, D. W. and Hummel, F. A., Synthesis and thermal expansion of polycrystalline cesium minerals. *J. Am. Ceram. Soc.*, 1972, **55**, 269–273.
10. Yanase, I., Hidehiko, H. and Mitamura, T., Thermal expansion property of synthetic cubic leucite-type compounds. *J. Ceram. Soc. Jpn.*, 2000, **108**, 26–31.
11. Taylor, D. and Henderson, C. M. B., The thermal expansion of the leucite group of minerals. *Am. Mineral.*, 1968, **53**, 1476–1489.
12. Beger, R. M., The crystal structure and chemical composition of pollucite. *Z. Kristallogr.*, 1969, **129**, 280–302.
13. Beall, G. H. and Ritter, H. L., Glass ceramics based on pollucite. *Adv. Ceram. Nucleation Crystallization Glasses*, 1982, **4**, 301–312.
14. Yanase, I., Tamal, S. and Kobayashi, H., Low-thermal-expansion property of sodium- and lithium-substituted cubic cesium leucite compounds. *J. Am. Ceram. Soc.*, 2003, **86**, 1360–1364.
15. Yanase, I., Tamal, S. and Kobayashi, H., Sintering of pollucite using amorphous powder and its low thermal expansion property. *J. Ceram. Soc. Jpn.*, 2003, **111**, 533–536.
16. Hildemann, L. M., Markowski, G. R., Jones, M. C. and Cass, G. R., Submicrometer aerosol mass distributions of emissions from boilers, fireplaces, automobiles, diesel trucks, and meat-cooking operation. *Aerosol Sci. Tech.*, 1991, **14**, 138–152.
17. Lin, J. J. and Lee, L.-C., Characterization of the concentration and distribution of urban submicron (PM1) aerosol particles. *Atmos. Environ.*, 2004, **38**, 469–475.
18. Ruiz, J. C., Blanc, Ph., Prouzet, E., Coryn, P., Laffont, P. and Larbot, A., Solid aerosol removal using ceramic filters. *Sep. Purif. Tech.*, 2000, **19**, 221–227.
19. Kobayashi, H., Terasaki, T., Mori, T., Yamamura, H. and Mitamiura, T., Preparation and thermal expansion behavior of pollucite powders by sol–gel processing. *J. Ceram. Soc. Jpn.*, 1991, **99**, 686–691.